Effect of adiabatic phonons on striped and homogeneous ground states

Yucel Yildirim[1,2] and Adriana Moreo[1]
[1]*Department of Physics and Astronomy, University of Tennessee, Knoxville, Tennessee 37966-1200, USA and Oak Ridge National Laboratory, Oak Ridge, Tennessee 37831-6032, USA*
[2]*Department of Physics and National High Magnetic Field Lab, Florida State University, Tallahassee, Florida 32306, USA*
(Received 8 March 2005; revised manuscript received 21 June 2005; published 20 October 2005)

The effects of adiabatic phonons on a spin-fermion model for high T_c cuprates are studied using numerical simulations. In the absence of electron-phonon interactions (EPI), stripes in the ground state are observed [C. Buhler, S. Yunoki, and A. Moreo, Phys. Rev. Lett. **84**, 2690 (2000); Phys. Rev. B. **62**, R3620 (2000)] for certain dopings while homogeneous states are stabilized in other regions of parameter space. Different modes of adiabatic phonons are added to the Hamiltonian: breathing, shear, and half-breathing modes. Diagonal and off-diagonal electron-phonon couplings are considered. It is observed that strong diagonal EPI generate stripes in previously homogeneous states, while in striped ground states an increase in the diagonal couplings tends to stabilize the stripes, inducing a gap in the density of states (DOS) and rendering the ground state insulating. The off-diagonal terms, on the other hand, destabilize the stripes creating inhomogeneous ground states with a pseudogap at the chemical potential in the DOS. The breathing mode stabilizes static diagonal stripes; while the half-breathing (shear) modes stabilize dynamical (localized) vertical and horizontal stripes. The EPI induces decoherence of the quasiparticle peaks in the spectral functions.

DOI: 10.1103/PhysRevB.72.134516 PACS number(s): 74.20.De, 74.25.Kc, 74.81.−g

I. INTRODUCTION

The pairing mechanism responsible for high T_c superconductivity is still unknown. The electron-phonon interactions that satisfactorily explain pairing for traditional superconductors within the BCS theory[2] would require phonon frequencies incompatible with the material stability in order to produce the observed high critical temperatures in the cuprates.[2] For this reason many researchers believe that magnetic interactions, which are observed in all the cuprates, may play an important role in the pairing mechanism.[3] As a result of this hypothesis, most of the Hamiltonians proposed to study the physics of the cuprates, such as the Hubbard and *t-J* models, only incorporate electronic and magnetic degrees of freedom.[4] However, experiments indicate that there are active phonon modes in the cuprates.[5–8] In addition, experimentally a very rich phase diagram, particularly in the underdoped regime, is starting to be unveiled. Some materials appear to have ground states with electronic stripes as observed in neutron scattering results,[8] while scanning tunneling microscopy indicates nanosize patches of superconducting and nonsuperconducting phases.[9,10] The emerging phase complexity is reminiscent of the experimental data for manganites where competing electronic, magnetic, and phononic degrees of freedom are responsible for the rich phase structure.[11]

For these reasons it is important to include electron-phonon interactions (EPI) in models for the cuprates. This would allow to understand whether EPI stabilize or destabilize charge stripes, what kind of inhomogeneous textures, if any, develop and, eventually, whether the interplay of magnetic and phonon interactions with the electrons is responsible for the pairing mechanism.[12]

The first step towards the goal of introducing EPI in models for the cuprates is to propose a simple but physically realistic Hamiltonian that can be studied with unbiased techniques. The proposals already in the literature include momentum dependent electron-phonon couplings that lead to long-range interactions in coordinate space[13,14] and/or quantum phonons which are very difficult to treat numerically.[15,16] Most studies have been performed using mean-field, slave-boson, or local density approximation (LDA).[17,18] Numerical simulations have been done using the *t-J* model in very small lattices, with a limited number of phonon modes and diagonal couplings,[15,16] or on the one-dimensional Hubbard model.[19]

In this paper we will study numerically a spin-fermion (SF) Hamiltonian for the cuprates[1] with electron-phonon interactions. The SF model is obtained as a simplification of the three band Hubbard model to a two band Hubbard model proposed by Emery[20] and a further simplification introduced by Loh *et al.*[21] This model reproduces many properties of the cuprates and presents stripes in the ground state, due solely to spin-charge interactions, in some regions of parameter space.[1] Thus, it provides a framework particularly suitable to study the effects of electron-phonon interactions on the preformed stripes. However, charge homogeneous ground states are also found in other regions of parameter space which allows to investigate charge inhomogeneity induced by EPI. Several phononic modes will be studied and diagonal and nondiagonal couplings, i.e., the dependence of the hopping and other Hamiltonian parameters on the lattice distortions, will be considered. The work will be performed in the adiabatic limit, i.e., at zero phononic frequency.

The paper is organized as follows: in Sec. II the Hamiltonian is introduced; the effect of electron-phonon interactions on striped states are presented in Sec. III, while Sec. IV is devoted to the effects of EPI on homogeneous states. Section V contains the conclusions.

II. THE MODEL

The SF model is constructed as an interacting system of electrons and spins, mimicking phenomenologically the coexistence of charge and spin degrees of freedom in the cuprates.[21,22] Its Hamiltonian is given by

$$H = -t\sum_{\langle \mathbf{ij}\rangle\alpha}(c^{\dagger}_{\mathbf{i}\alpha}c_{\mathbf{j}\alpha}+\text{h.c.}) + J\sum_{\mathbf{i}}\mathbf{s_i}\cdot\mathbf{S_i} + J'\sum_{\langle \mathbf{ij}\rangle}\mathbf{S_i}\cdot\mathbf{S_j}, \quad (1)$$

where $c^{\dagger}_{\mathbf{i}\alpha}$ creates an electron at site $\mathbf{i}=(i_x,i_y)$ with spin projection α, $\mathbf{s_i}=\Sigma_{\alpha\beta}c^{\dagger}_{\mathbf{i}\alpha}\sigma_{\alpha\beta}c_{\mathbf{i}\beta}$ is the spin of the mobile electron, the Pauli matrices are denoted by σ, $\mathbf{S_i}$ is the localized spin at site $\mathbf{i}$, $\langle \mathbf{ij}\rangle$ denotes nearest-neighbor (NN) lattice sites, t is the NN-hopping amplitude for the electrons, $J>0$ is an antiferromagnetic (AF) coupling between the spins of the mobile and localized degrees of freedom, and $J'>0$ is a direct AF coupling between the localized spins. The density $\langle n\rangle=1-x$ of itinerant electrons is controlled by a chemical potential μ. Hereafter $t=1$ will be used as the unit of energy. J' and J are fixed to 0.05 and 2.0, respectively, values shown to be realistic in previous investigations.[1] The temperature will be fixed to a low value: $T=0.01$, which was shown before to lead to the correct high-T_c phenomenology.[1,23] Periodic boundary conditions will be used but the results, particularly stripe formation, are similar with open boundary conditions.[1] Good agreement with experimental results has been obtained for $t=0.5$ eV.[24]

The diagonal electron-phonon part of the Hamiltonian being proposed here is given by

$$H^{(j)}_{\text{e-ph}} = -\lambda\sum_{\mathbf{i}} Q^{(j)}_{\mathbf{i}} n_{\mathbf{i}}, \quad (2)$$

where $n_{\mathbf{i}}=\Sigma_{\sigma}c^{\dagger}_{\mathbf{i}\sigma}c_{\mathbf{i}\sigma}$ is the electronic density on site $\mathbf{i}$ and $Q^{(j)}_{\mathbf{i}}$ is the phonon mode defined in terms of the lattice distortions $u_{\mathbf{i},\alpha}$ which measures the displacement along the directions $\alpha=\hat{x}$ or $\hat{y}$ of oxygen ions located at the center of the lattice's links in the equilibrium position, i.e., $u_{\mathbf{i},\alpha}=0$. The index (j) identifies the phonon mode. In this work, the following phonon modes will be considered.

(a) The *breathing* mode given by

$$Q^{(1)}_{\mathbf{i}} = \sum_{\alpha}(u_{\mathbf{i},\alpha} - u_{\mathbf{i}-\hat{\alpha},\alpha}); \quad (3)$$

(b) The *shear* mode, in which the oxygens along, e.g., x move in counterphase with the oxygens along y, given by

$$Q^{(2)}_{\mathbf{i}} = \sum_{\alpha}(-1)^{\sigma}(u_{\mathbf{i},\alpha} - u_{\mathbf{i}-\hat{\alpha},\alpha}), \quad (4)$$

with $\sigma=1(-1)$ for $\alpha=x(y)$;

(c) The *half-breathing* mode along x given by

$$Q^{(3)}_{\mathbf{i}} = (u_{\mathbf{i},x} - u_{\mathbf{i}-\hat{\mathbf{x}},x}); \quad (5)$$

and (d) The *half-breathing* mode along y given by

$$Q^{(4)}_{\mathbf{i}} = (u_{\mathbf{i},y} - u_{\mathbf{i}-\hat{\mathbf{y}},y}). \quad (6)$$

Note that although the proposed interactions seem local in coordinate space, they correspond to cooperative lattice distortions which, in turn, will produce strongly momentum dependent effective electron-phonon couplings, in agreement with the experimental evidence observed in the cuprates.[6]

A term to incorporate the stiffness of the Cu–O bonds is added. The term bounds the amplitude of the lattice distortions induced by $H_{\text{e-ph}}$. Its explicit form is

$$H_{\text{ph}} = \kappa\sum_{\mathbf{i},\alpha}(u_{\mathbf{i},\alpha})^2, \quad (7)$$

where κ is the stiffness parameter that will be set to 1 here. In addition, we will consider the off-diagonal interactions induced by the lattice distortions. To obtain these terms we follow the approach of Ishihara *et al.*[19,18] As a result the hopping t in Eq. (1) now becomes site and direction dependent and it is given by

$$t_{\mathbf{i},\mathbf{j}} = t + \gamma[u(\mathbf{i}) + u(\mathbf{j})], \quad (8)$$

where γ is a parameter and

$$u(\mathbf{i}) = u_{\mathbf{i},x} - u_{\mathbf{i}-\hat{\mathbf{x}},x} + u_{\mathbf{i},y} - u_{\mathbf{i}-\hat{\mathbf{y}},y}. \quad (9)$$

The Heisenberg coupling J' in Eq. (1) also is affected by the lattice distortions and it has to be replaced by

$$J'_{\mathbf{i},\mathbf{j}} = J' + g_J\gamma[u(\mathbf{i}) + u(\mathbf{j})], \quad (10)$$

where g_J is another parameter.

As stated above, the spin-fermion model with electron-phonon interactions will be studied with a Monte Carlo (MC) algorithm. To simplify the numerical calculations, avoiding the sign problem, the localized spins are assumed to be classical (with $|\mathbf{S_i}|=1$). This approximation is not drastic since most of the high T_c phenomenology is reproduced in this limit, and it was already discussed in detail in Ref. 1. Details of the MC method can be found in Ref. 25. Square lattices with 8×8 and 12×12 sites will be studied here.

III. INFLUENCE OF PHONONS ON STRIPED STATES

Neutron scattering experiments have shown that doping causes magnetic incommensuration in the cuprates.[26,27] The origin of this phenomenon is still being debated. One possible scenario is the formation of charge stripes in the ground state upon doping.[28,29] Experiments on nickelates such as $La_{2-x}Sr_xNiO_4$ (LSNO) have shown the presence of diagonal static stripes[8] and there is evidence of stripes also in LNSCO, i.e., Nd doped $La_{2-x}Sr_xCuO_4$ (LSCO) (Ref. 30) and in $La_{2-x}Ba_xCuO_4$ (LBCO).[31] It is conjectured that the magnetic incommensurability observed in other high T_c cuprates is due to the presence of dynamical stripes and that the stripe dynamics may be related to the electron-phonon couplings in the different materials. Despite these theoretical scenarios, it has been very difficult to find striped ground states in models for the cuprates when studied with unbiased techniques. Stripes have been observed in the t-J model[32,33] but they are difficult to stabilize and it is not clear whether the striped state is the actual ground state or a very low lying excited one. Stripes, on the other hand, have been obtained without biases in the SF model that will be studied in this work.[1] This characteristic will allow us to explore the effect of electron-phonon interactions in striped ground states. The charge tex-

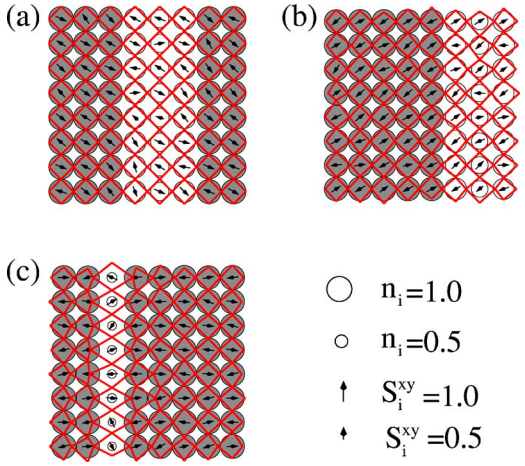

FIG. 1. (Color online) (a) MC snapshot of an 8×8 lattice at $\langle n\rangle=0.875$ for $\lambda=0$ and $\gamma=0$. The size of the circles is proportional to the electronic density; the shaded circles have charge density larger than the average, i.e., $n_i\geqslant\langle n\rangle=0.875$. The arrows represent the projection of the localized spins in the plane x-y; the lines indicate lattice distortions (see text); (b) same as (a) but for $\lambda=1$ and mode $Q^{(2)}$; (c) same as (b) but for $\lambda=2$.

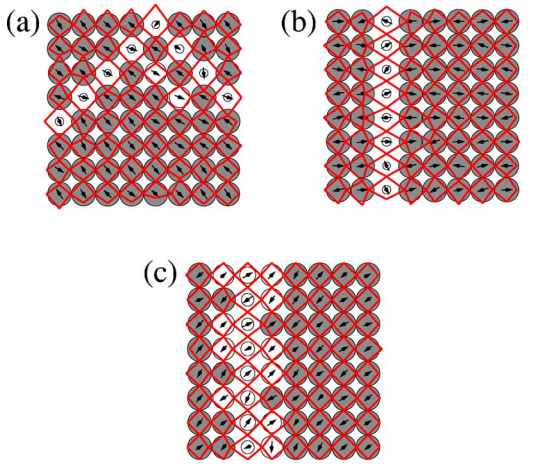

FIG. 2. (Color online) (a) MC snapshot of an 8×8 lattice at $\langle n\rangle=0.875$, for mode $Q^{(1)}$, $\lambda=2$ and $\gamma=0$; (b) same as (a) but for mode $Q^{(2)}$; (c) same as (a) but for mode $Q^{(3)}$.

ture will be monitored by measuring the density structure factor $N(\mathbf{q})$.[1] The magnetic structure factor $S(\mathbf{q})$ will provide information on the magnetic properties. Lattice distortions will be monitored by measuring correlations between the displacements, although the development of long range correlations in the lattice degrees of freedom is not anticipated.

The dynamic properties of the system will be monitored by measuring the density of states $N(\omega)$ and the one-particle spectral functions $A(\mathbf{q},\omega)$ and the optical conductivity $\sigma(\omega)$.[1,23]

A. Diagonal electron-phonon term

In our investigations it has been observed that in general the diagonal electron-phonon interaction plays a stabilizing role on stripe structures. This behavior was obtained for the four phonon modes studied here. For $0\leqslant\lambda\leqslant2$ the holes become more localized in the stripes as λ increases. This can be seen in Fig. 1, where snapshots for $\langle n\rangle=0.875$ are displayed for $\lambda=0$ [Fig. 1(a)], $\lambda=1$ [Fig. 1(b)], and $\lambda=2$ [Fig. 1(c)]. The lines in the snapshots indicate the lattice distortions. If all the displacements $u_{\mathbf{i},\alpha}$ were 0 then, the lines would cross at the middle point of the links that join the lattice sites [as in Fig. 1(a)]. Out of center crossings indicate ionic displacements. It is clear from the figure that, as λ increases, lattice distortions in the direction perpendicular to the stripe develop along the stripe with the mode $Q^{(2)}$, further localizing it. In Fig. 1(c) large displacements along the horizontal direction can be seen in the links next to the stripe. The stripes become thinner and the density of holes per site inside the stripes increases.

We have observed some differences between the effects of the various phonon modes studied here as the strength of the diagonal electron-phonon coupling λ increases. In Fig. 2 snapshots for $\lambda=2$ at $\langle n\rangle=0.875$ are presented for $Q^{(1)}$, $Q^{(2)}$, and $Q^{(3)}$.[34] A clear tendency to form *diagonal* stripes is seen for the breathing mode $Q^{(1)}$ [Fig. 2(a)]. Since in this case holes are localized by being surrounded by four elongated bonds they cannot be accommodated in vertical or horizontal formations. Note that the single stripe that is stable at $\lambda=0$ for the electronic density shown in Fig. 2 gets destabilized due to the $Q^{(1)}$ strong electron-phonon coupling. This result agrees with the fact that diagonal stripes are observed in LSNO and experiments indicate that the breathing mode is the mode most strongly coupled to the electrons.[35] According to our results, a robust diagonal coupling of the electrons to the breathing mode should be expected in the nickelates.

In Fig. 2(b) it can be observed that the shear mode $Q^{(2)}$ tends to stabilize vertical (or horizontal) stripes because a large horizontal (or vertical) distortion occurs, localizing the holes along the stripe. Interestingly, the half-breathing mode also produces vertical (or horizontal) stripes but the holes are less localized since the lattice can distort only along the horizontal (or vertical) direction. As a result, more dynamical stripes are observed for the half-breathing modes even for strong diagonal electron-phonon couplings [Fig. 2(c)]. Notice that the experimental evidence indicates that in LNSCO, where vertical and horizontal stripes are observed, the mode more strongly coupled to the electrons is the half-breathing mode.[6]

Another indication of increasing localization with increasing λ is observed in the peak in $N(\mathbf{q})$, at $\mathbf{q}=(\pi/4,0)$ for the stripes shown in Figs. 1(a)–1(c), which becomes better developed as λ increases [Fig. 3(a)]. In addition, the pseudogap in the density of states at the chemical potential becomes a full gap indicating an increase in insulating behavior [Fig. 3(b)].

Similar results are obtained at $\langle n\rangle=0.75$ for which two stripes are stabilized, even at $\lambda=0$, in the 8×8 systems studied here.

The general trend, for different electronic densities and phonon modes, is that the ground state becomes more insulating as the diagonal electron-phonon coupling increases. The shear mode $Q^{(2)}$ will be used as an example but similar qualitative behavior is observed for the other modes. In Fig.

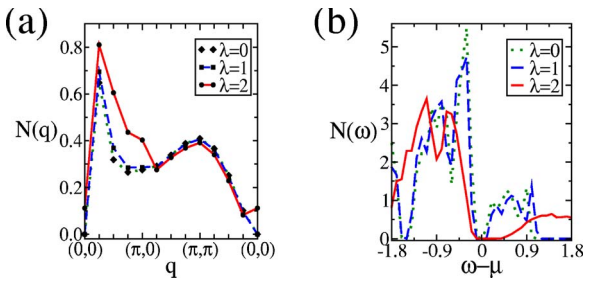

FIG. 3. (Color online) (a) The charge structure factor $N(\mathbf{q})$ for various values of λ for the same parameters as in Fig. 1; (b) The density of states $N(\omega)$ for several values of the diagonal electron-phonon coupling λ, for the same parameters as in (a). The phonon mode is $Q^{(2)}$.

4(a) it can be seen that the spectral weight at $\omega=0$ in the density of states decreases with increasing λ for different values of the electronic density $\langle n\rangle$. The Drude weight, shown in Fig. 4(b), also decreases and insulating behavior is obtained for all densities at $\lambda=2$.

Although the effect of charge localization with increasing λ is more pronounced at densities for which stripes are observed, we see in the snapshots shown in Fig. 5 for $\langle n\rangle=0.8$ and mode $Q^{(2)}$ that the charge becomes more localized as λ increases and the lattice distortions localizing the holes develop large values for $\lambda\approx 2$. Note that AF domains separated by walls of holes are observed. These inhomogeneous structures appear to replace the stripes when the density of holes is not commensurate with the lattice size. An important characteristic of these inhomogeneous states is that, although no features are observed in the charge structure factor $N(\mathbf{q})$, incommensurate magnetic correlations are still present and the peaks in $S(\mathbf{q})$ occur at $(\pi,\pi-\delta)$ and $(\pi-\delta,\pi)$, i.e., in qualitative agreement with the incommensurate peaks observed in the cuprates.

In the configurations shown in Fig. 5, $S(\mathbf{q})$ has a maximum at $\mathbf{q}=(\pi,3\pi/4)$ for snapshot (a), but there is also a less intense peak at $\mathbf{q}=(3\pi/4,\pi)$.

Incommensurate peaks in $S(\mathbf{q})$ at $\mathbf{q}=(\pi,3\pi/4)$ and $\mathbf{q}=(3\pi/4,\pi)$ with almost equal weight are observed for $\langle n\rangle=0.8$ and $\lambda=1$ [see Fig. 5(d)] although no peak in $N(\mathbf{q})$ is observed. In Fig. 5(b) the snapshot of the final configuration

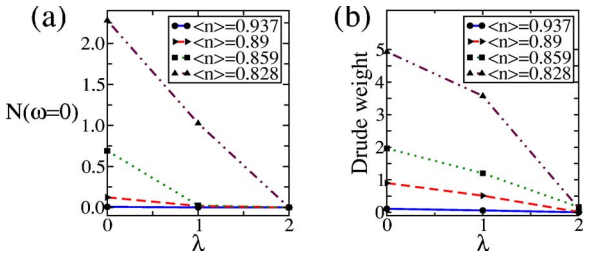

FIG. 4. (Color online) (a) Spectral weight in the density of states $N(\omega)$ at $\omega=0$ as a function of the diagonal electron-phonon coupling λ for several values of the electronic density $\langle n\rangle$ and mode $Q^{(2)}$; (b) Drude weight as a function of the diagonal electron-phonon coupling λ for several values of the electronic density $\langle n\rangle$ and mode $Q^{(2)}$.

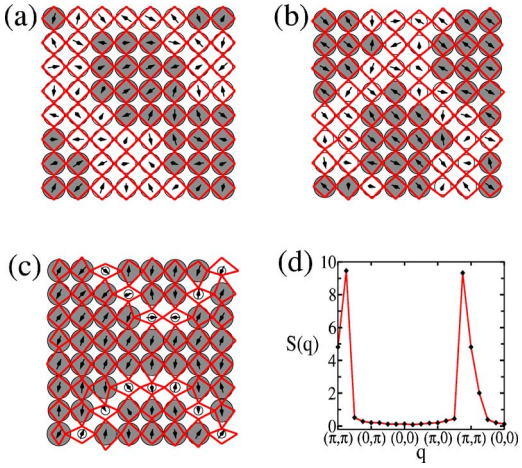

FIG. 5. (Color online) (a) MC snapshot of an 8×8 lattice at $\langle n\rangle=0.8$ $\lambda=0$ and $\gamma=0$; (b) same as (a) but for $\lambda=1$ with mode $Q^{(2)}$; (c) same as (b) for $\lambda=2$; (d) Magnetic structure factor for the parameters in (b).

of the corresponding Monte Carlo run is shown. Other snapshots of configurations appearing during the measuring part of our simulation are displayed in Fig. 6. It can be seen that the ground state is not frozen and that there is a dynamical charge redistribution. Thus, the magnetic incommensurability observed in some cuprates could be due to charge and spin configurations similar to those presented in Fig. 6, which could be interpreted as "dynamic stripes." In fact, these results may indicate that the patches in Figs. 5 and 6 are not random islands since, if that were the case, we would expect that the maxima in $S(\mathbf{q})$ would form a ring in momentum space.[36] It is tempting to associate the observed patches with "dynamical" stripes. Notice that for the states with "static" stripes only one peak at $\mathbf{q}=(\pi,\pi-\delta)$ is observed in $S(\mathbf{q})$ if the peak in $N(\mathbf{q})$ is at $\mathbf{q}=(0,2\delta)$. On the other hand, the states with dynamical stripes naturally reproduce the four peaks observed in neutron scattering experiments for the

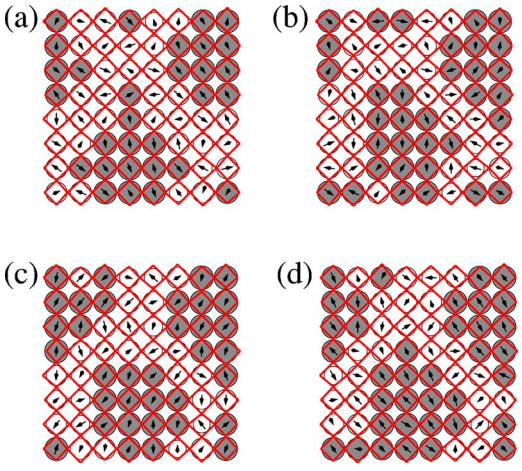

FIG. 6. (Color online) (a) MC snapshot of an 8×8 lattice at $\langle n\rangle=0.8$, for mode $Q^{(2)}$, $\lambda=1$ and $\gamma=0$, after 2600 measuring sweeps; (b) same as (a) but after 3750 measuring sweeps; (c) same as (a) but after 4250 measuring sweeps; (d) same as (a) but after 5000 measuring sweeps.

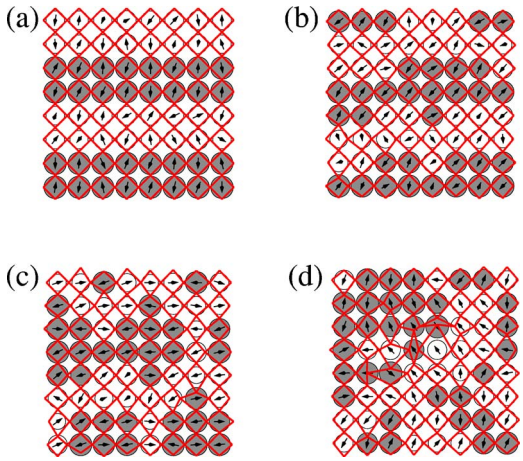

FIG. 7. (Color online) Study of the effect of off-diagonal couplings. (a) MC snapshot of an 8×8 lattice at $\langle n\rangle=0.75$, $\lambda=0$, and $\gamma=0$; (b) same as (a) but for $\gamma=0.1$ and mode $Q^{(2)}$; (c) same as (b) for $\gamma=0.2$; (d) same as (b) but for $\gamma=0.6$.

cuprates[26,27] and the "patchlike" shape of the clusters would explain, at the same time, the apparently random inhomogeneous structures observed in scanning tunneling microscopy (STM) experiments.[9,10]

As the diagonal electron-phonon coupling λ increases beyond $\lambda=2$, important quantitative changes are observed, in particular, the tendency to bipolaron formation induced by strong lattice distortions. This behavior will be discussed in more detail in Sec. III C.

B. Off-diagonal electron-phonon term

In this first exploratory study of the effects of the off-diagonal terms due to the EPI we will allow the parameter γ in Eqs. (8) and (10) to vary in the interval (0, 0.6), while g_J [see Eq. (10)] will be kept equal to 1. In general, we have observed that the effect of the off-diagonal term is to destabilize the stripes, since they become more dynamic. Examples of this effect can be seen in the snapshots presented in Fig. 7 for $\langle n\rangle=0.75$ and $\gamma=0$, 0.1, 0.2, and 0.6. The stripes become distorted as γ increases and, eventually, AF domains separated by irregularly shaped hole-rich regions start to develop.

In Fig. 8(a), it is shown how the sharp maximum in the charge structure factor loses intensity as the stripes become more dynamic. However, notice that the magnetic structure factor [Fig. 8(b)] still shows incommensurability at $\mathbf{q}=(\pi,3\pi/4)$ which is in agreement with neutron scattering data for dynamic stripes. For $\gamma\geq0.4$ a peak in $S(\mathbf{q})$ develops at $\mathbf{q}=(0,0)$. This seems to occur because the hole domains become ferromagnetic as it can be seen in Figs. 7(c) and 7(d).

The system also becomes more metallic since the Drude weight increases with γ [Fig. 8(c)] and more spectral weight appears in the pseudogap in the density of states (DOS) [Fig. 8(d)].

C. Diagonal and off-diagonal terms

When both diagonal and nondiagonal electron-phonon couplings are active simultaneously, we have observed that

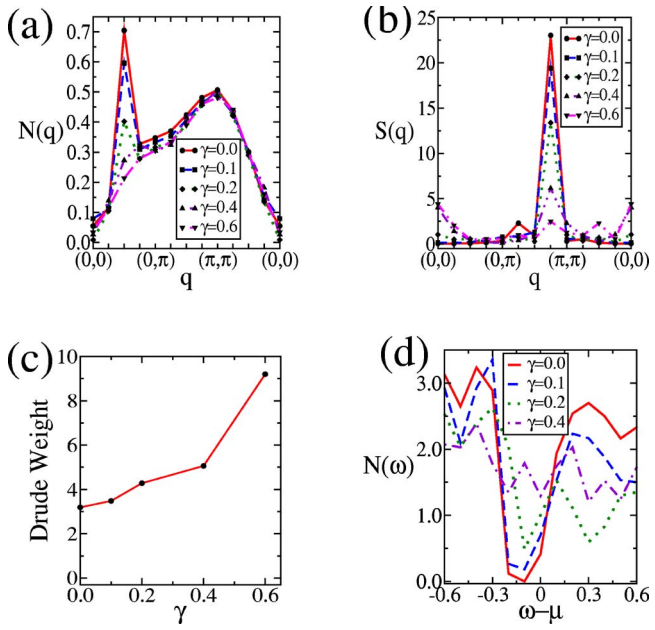

FIG. 8. (Color online) (a) Charge structure factor for different values of γ (strength of the off-diagonal EPI) and for $\lambda=0$ on an 8×8 lattice at $\langle n\rangle=0.75$, for mode $Q^{(2)}$; (b) the magnetic structure factor for the same parameters as in (a); (c) the Drude weight for the same parameters as in (a); (d) the density of states for the same parameters as in (a).

for values of $\lambda\leq2$, there is a competition between the localizing effect of the diagonal electron-phonon coupling λ and the disordering tendency of the off-diagonal parameter γ. As a result, larger values of γ than in the case of $\lambda=0$ are needed to destabilize the stripes. The stripe states are replaced by AF "clusters" separated by hole-rich regions as shown in Fig. 9.

We also have observed that for $\lambda\geq3$ the modes $Q^{(1)}$ and $Q^{(2)}$ induce charge density wave (CDW) states. CDW domains are formed in order to accommodate the extra holes

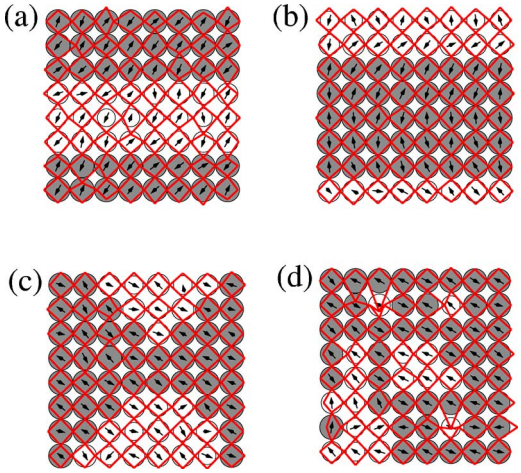

FIG. 9. (Color online) (a) MC snapshot of an 8×8 lattice at $\langle n\rangle=0.875$, for mode $Q^{(2)}$, $\lambda=1$, and $\gamma=0$; (b) same as (a) but for $\gamma=0.1$; (c) same as (a) but for $\gamma=0.2$; (d) same as (a) but for $\gamma=0.4$.

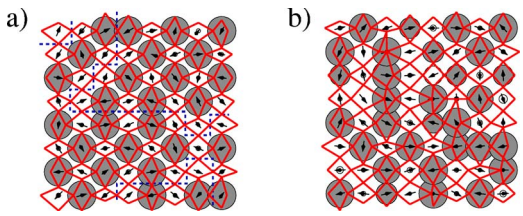

FIG. 10. (Color online) (a) MC snapshot of an 8×8 lattice at $\langle n\rangle=0.875$, for mode $Q^{(2)}$, $\lambda=6$, and $\gamma=0$. The dashed lines separate CDW domains; (b) same as (a) but for $\gamma=0.2$.

away from half-filling as shown in Fig. 10(a) for $\langle n\rangle=0.875$ and mode $Q^{(2)}$. This is the only case in which we have observed long range order developing in the lattice degrees of freedom. The dashed lines in the figure indicate different CDW domains. In Fig. 10(b) it can be seen how the off-diagonal coupling destabilizes the CDW state and a disordered state with bipolarons (two electrons trapped at the same site) is observed.

As γ increases the off-diagonal term opposes the trend towards bipolaron formation caused by the diagonal electron-phonon coupling and stripelike structures reappear for some dopings.

The half-breathing modes, on the other hand, are not able to stabilize a CDW state even for large values of diagonal couplings and they only produce disordered states with bipolarons when the diagonal electron-phonons coupling is large. Since CDW and superconducting states normally compete with each other, the half-breathing mode may enhance the development of superconductivity. Unfortunately, off-diagonal long-range order which characterizes S or D wave superconductivity, cannot develop with adiabatic phonons.[37] Thus, this possibility should be explored for finite values of the frequency of the lattice vibrations in a full quantum calculation.

D. Spectral functions

In this subsection the properties of the spectral functions $A(\mathbf{q},\omega)$ will be discussed in detail.

Numerical studies of the spin-fermion model without phonons in Ref. 23 have shown that the underdoped regime is characterized by a depletion of spectral weight along the diagonal direction in momentum space, where a very weak Fermi surface (FS) may exist. On the other hand, strong spectral weight, very flat bands, and a well defined FS are observed close to $\mathbf{q}=(\pi,0)$ and $(0,\pi)$. These results are in agreement with ARPES studies for LSCO,[38] material believed to have dynamic stripes, and also with numerical studies of models in which stripes have been built via a configuration dependent "stripe" potential in the t-J model[39] or with stripelike mean-field states.[40] ARPES results for LNSCO, where stripes have been observed,[30] indicate that the low-energy excitation near the expected d-wave node region is strongly suppressed.[41]

In the absence of EPI the above mentioned characteristics are well reproduced by the SF model. In Fig. 11(a) the spectral function $A(\mathbf{q},\omega)$ along the path $\mathbf{q}=(0,0)-(\pi,0)-(\pi,\pi)$ for $\langle n\rangle=0.80$ on a 12×12 lattice in the absence of EPI is presented. A well defined quasi-particle peak is observed at (0, 0), a flatband appears close to $(\pi,0)$ and the peak crosses the Fermi energy at $(\pi,5\pi/6)$ defining a hole-like FS. The spectral function along the diagonal of the Brillouin zone is presented in Fig. 11(b). It can be seen how the spectral weight becomes very incoherent as the Fermi energy is reached.

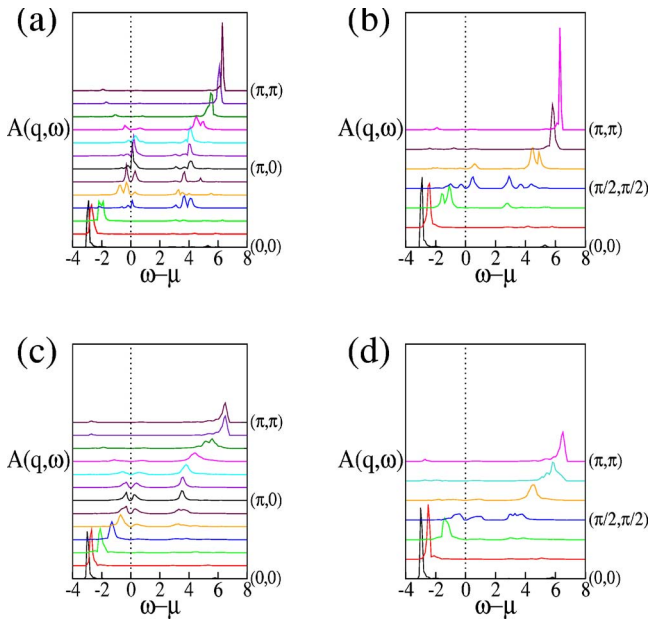

FIG. 11. (Color online) (a) Spectral functions along the path $\mathbf{q}=(0,0)-(\pi,0)-(\pi,\pi)$ on a 12×12 lattice at $\langle n\rangle=0.8$, $\lambda=0$, and $\gamma=0$; (b) same as (a) but along the diagonal direction in the Brillouin zone; (c) same as (a) but for $\lambda=2$ and mode $Q^{(3)}$; (d) same as (b) but for $\lambda=2$.

As a general rule we have observed that electron-phonon interactions increase the decoherence of the spectral functions, particularly close to the Fermi energy. Below, we will discuss the effects of the different phonon modes for the most interesting case of dynamic stripes (see, for example, Fig. 6).

The diagonal electron-phonon coupling renders the system insulator, as discussed in Sec. III A. In Fig. 11(c) the spectral weight along the path $\mathbf{q}=(0,0)-(\pi,0)-(\pi,\pi)$ is displayed for $\lambda=2$ and the half-breathing mode $Q^{(3)}$ in a 12×12 lattice. It can be seen that the quasiparticles are less well defined and that a clear gap has opened at the Fermi energy. Along the diagonal of the Brillouin zone [Fig. 11(d)] the spectral weight becomes more incoherent and a gap also is observed.

The off-diagonal EPI restores spectral weight in the gap but there are no quasiparticles close to the Fermi energy as it can be seen in Figs. 12(a) and 12(b) where the spectral functions for $\lambda=2$, $\gamma=0.4$, and mode $Q^{(3)}$ are shown along $\mathbf{q}=(0,0)-(\pi,0)-(\pi,\pi)$ and along the diagonal of the Brillouin zone. For γ finite and $\lambda=0$ the only observed changes is that the peaks in Figs. 11(a) and 11(b) become broader.

For $\lambda=2$ the breathing mode creates a larger insulating gap than the half-breathing mode and produces a larger de-

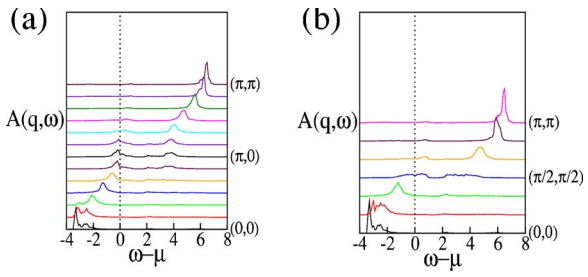

FIG. 12. (Color online) (a) Spectral functions along the path $\mathbf{q}=(0,0)-(\pi,0)-(\pi,\pi)$ on a 12×12 lattice at $\langle n\rangle=0.8$, $\lambda=2$, and $\gamma=0.4$ for the half-breathing mode; (b) same as (a) but along the diagonal direction in the Brillouin zone.

coherence of the quasiparticle peaks. The results for the shear mode are qualitatively very similar.

The off-diagonal EPI for the shear and breathing modes tends to close the gap and increase the decoherence.

IV. INFLUENCE OF PHONONS ON HOMOGENEOUS STATES AND GENERATION OF STRIPES

Up to this point we have considered the effects of EPI on ground states that already presented charge inhomogeneity. However, it is important to study whether the electron-phonon interactions proposed in this work can themselves generate charge inhomogeneity, in particular stripes, in a previously homogeneous ground state.

In order to address this issue, we studied the SF model with $J=1.5$ instead of $J=2$, value which was used in the previous sections (all the other parameters are kept the same). For $\langle n\rangle=0.75$ the ground state has an homogeneous charge distribution as it can be observed in the MC snapshot presented in Fig. 13(a). Note that despite the charge homogeneity this state presents magnetic incommensurability due to a spiral spin arrangement in the vertical direction.

One of the main results of this paper is our observation that a strong diagonal coupling with the shear mode *generates* two horizontal or vertical stripes. An example can be seen in the snapshot presented in Fig. 13(b) for $\lambda=2$. In this case the holes act as boundaries between undoped antiferromagnetic states and the magnetic incommensurability arises from the inhomogeneous charge distribution. A π-shift among the AF domains is observed as well.[42]

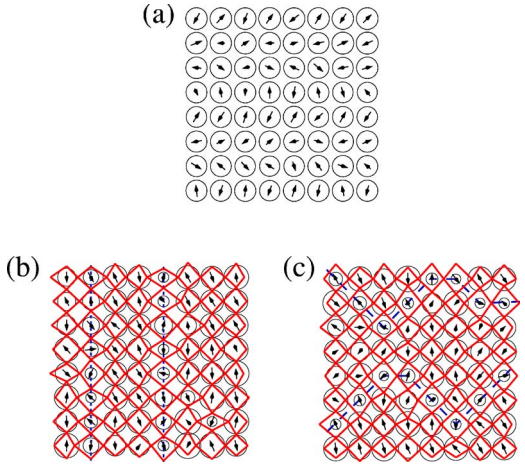

FIG. 13. (Color online) (a) MC snapshot of an 8×8 lattice at $\langle n\rangle=0.75$, $J=1.5$, $\lambda=0$, and $\gamma=0$; (b) same as (a) but for $\lambda=2$ with mode $Q^{(2)}$; (c) same as (b) with mode $Q^{(1)}$. The dashed line indicates the stripes.

The breathing mode also induces charge inhomogeneity for a diagonal coupling $\lambda=2$. From the discussion in Sec. III A diagonal stripes would be expected but we have observed two stripes with a zig-zag shape, i.e., the holes align diagonally at short distance scales but, on the whole, the stripe is still horizontal or vertical [see Fig. 13(c)].

This result indicates that *diagonal EPI are able to induce stripelike charge inhomogeneities in otherwise homogeneous states*. However, the SF model also shows that although diagonal EPI stabilize stripes they are not *necessary* to induce them. Charge inhomogeneities can result even in the absence of EPI, just from magnetic interactions.

V. CONCLUSIONS

Summarizing, we have studied the effects of diagonal and off-diagonal electron-phonon interactions using nonbiased numerical techniques on a model that has both striped and homogeneous ground states in the absence of EPI. We found that diagonal EPI tend to either generate or further stabilize the existing stripes and turn the system into an insulator. Horizontal and vertical stripes are stabilized by half-breathing and shear modes, but the stripes generated by shear modes are more localized. The breathing mode stabilizes static diagonal stripes for intermediate diagonal couplings. Large diagonal couplings stabilize CDW states for breathing and shear modes but this state is not observed with the half-breathing mode. Actual values of the diagonal hopping can be estimated using $t=0.5$ eV. From the studies presented in this paper, $\lambda\approx2$ eV would be necessary to produce very localized stripes while CDW states will appear for unrealistically large values, $\lambda\geqslant6$ eV.

On the other hand, off-diagonal electron-phonon couplings destabilize the stripes making the ground state more metallic, although nonhomogeneous. Instead of static stripes other kinds of inhomogeneous structures characterized by antiferromagnetic domains separated by barriers of holes are observed. Notice that our investigations suggest that off-diagonal couplings as small as 0.05 eV are sufficient to produce dynamic stripes.

The electron-phonon interactions undermine the quasiparticle peaks in the spectral functions close to the Fermi energy producing incoherent weight. Breathing and shear modes tend to open large gaps at the Fermi energy creating insulating behavior. The half-breathing mode, on the other hand, opens smaller gaps that are closed by relatively modest off-diagonal couplings, allowing for metallic behavior.

Our results indicate that the half-breathing mode is most likely to play a role in noninsulating materials with vertical and/or horizontal dynamic stripes, such as LSCO, while the breathing mode should dominate on insulators with diagonal stripes like the nickelates.

The most important result of this study is the fact that different phonon modes promote a diverse array of charge structures and that the relative strength of diagonal and off-diagonal couplings influences the transport properties. Diagonal electron-phonon couplings promote insulating behavior, while off-diagonal interactions are crucial to achieve metallicity. It appears that the half-breathing mode off-diagonally coupled to the electrons is the most likely to produce noninsulating states with dynamical stripes as observed in the cuprates. This is in agreement with the experimental data which indicate the prevalence of half-breathing modes in the high T_c cuprates.[6] The electron-phonon interaction introduces decoherence of the quasiparticle peak in the spectral function in agreement with ARPES measurements in LSCO.

The crucial issue that remains to be explored is whether electron-phonon interactions are needed, in addition to the magnetic exchange, in order to develop long range D-wave pairing correlations. Since superconductivity arises from off-diagonal long range order, it cannot be generated with adiabatic phonons. The next step will be to study off-diagonally coupled half-breathing modes at finite frequencies.

ACKNOWLEDGMENTS

We acknowledge discussions with T. Egami, J. Tranquada, G. Sawatsky, and E. Dagotto. A.M. is supported by NSF under Grant Nos. DMR-0443144 and DMR-0454504. Additional support is provided by ORNL.

[1] C. Buhler, S. Yunoki, and A. Moreo, Phys. Rev. Lett. **84**, 2690 (2000); Phys. Rev. B **62**, R3620 (2000).
[2] J. Bardeen, L. N. Cooper, and J. R. Schrieffer, Phys. Rev. **108**, 1175 (1957).
[3] P. W. Anderson and J. R. Schrieffer, Phys. Today **44** (6), 54 (1991).
[4] E. Dagotto, Rev. Mod. Phys. **66**, 763 (1994).
[5] A. Bianconi, N. L. Saini, A. Lanzara, M. Missori, T. Rossetti, H. Oyanagi, H. Yamaguchi, K. Oka, and T. Ito, Phys. Rev. Lett. **76**, 3412 (1996).
[6] R. J. McQueeney, Y. Petrov, T. Egami, M. Yethiraj, G. Shirane, and Y. Endoh, Phys. Rev. Lett. **82**, 628 (1999).
[7] A. Lanzara, P. V. Bogdanov, X. J. Zhou, S. A. Kellar, D. L. Feng, E. D. Lu, S. Uchida, H. Eisaki, A. Fujimori, K. Kishio, J.-I. Shimoyama, T. Noda, S. Uchida, Z. Hussain, and Z.-X. Shen, Nature (London) **412**, 510 (2001).
[8] J. M. Tranquada, D. J. Buttrey, V. Sachan, and J. E. Lorenzo, Phys. Rev. Lett. **73**, 1003 (1994); J. M. Tranquada, R. Mallozi, J. Orenstein, T. N. Eckstein, and I. Bozovic, Nature (London) **375**, 561 (1995).
[9] K. McElroy, R. W. Simmonds, J. E. Hoffman, D.-H. Lee, J. Orenstein, H. Eisaki, S. Uchida, and J. C. Davis, Nature (London) **422**, 520 (2003).
[10] M. Vershinin, S. Misra, S. Ono, Y. Abe, Y. Ando, and A. Yazdani, www.sciencexpress.org, 10.1126/science.1093384.
[11] E. Dagotto, T. Hotta, and A. Moreo, Phys. Rep. **344**, 1 (2001).
[12] T. Egami and S. Billinge, in *Physical Properties of High Temperature Superconductors V*, edited by D. M. Ginsberg (World Scientific, Singapore, 1996), p. 265.
[13] O. Rösch and O. Gunnarsson, Phys. Rev. Lett. **92**, 146403 (2004).
[14] T. P. Devereaux, T. Cuk, Z.-X. Shen, and N. Nagaosa, Phys. Rev. Lett. **93**, 117004 (2004).
[15] A. Dobry, A. Greco, S. Koval, and J. Riera, Phys. Rev. B **52**, 13722 (1995).
[16] T. Sakai, D. Poilblanc, and D. J. Scalapino, Phys. Rev. B **55**, 8445 (1997).
[17] K. Yonemitsu, A. R. Bishop, and J. Lorenzana, Phys. Rev. B **47**, 8065 (1993).
[18] S. Ishihara and N. Nagaosa, Phys. Rev. B **69**, 144520 (2004).
[19] S. Ishihara, T. Egami, and M. Tachiki, Phys. Rev. B **55**, 3163 (1997); Y. Petrov and T. Egami, *ibid.* **58**, 9485 (1998).
[20] V. J. Emery, Phys. Rev. Lett. **58**, 2794 (1987).
[21] E. Y. Loh, Jr., T. Martin, P. Prelovsek, and D. K. Campbell, Phys. Rev. B **38**, 2494 (1988).
[22] A. V. Chubukov, Phys. Rev. B **52**, R3840 (1995); S. Klee and A. Muramatsu, Nucl. Phys. B **473**, 539 (1996); J. R. Schrieffer, J. Low Temp. Phys. **99**, 397 (1995); B. L. Altshuler, L. B. Ioffe, and A. J. Millis, Phys. Rev. B **52**, 5563 (1995); C.-X. Chen and H.-B. Schuttler, *ibid.* **43**, 3771 (1991).
[23] M. Moraghebi, C. Buhler, S. Yunoki, and A. Moreo, Phys. Rev. B **63**, 214513 (2001).
[24] M. Moraghebi, S. Yunoki, and A. Moreo, Phys. Rev. B **66**, 214522 (2002).
[25] E. Dagotto, S. Yunoki, A. L. Malvezzi, A. Moreo, J. Hu, S. Capponi, D. Poilblanc, and N. Furukawa, Phys. Rev. B **58**, 6414 (1998).
[26] T. E. Mason, G. Aeppli, and H. A. Mook, Phys. Rev. Lett. **68**, 1414 (1992).
[27] S.-W. Cheong, G. Aeppli, T. E. Mason, H. Mook, S. M. Hayden, P. C. Canfield, Z. Fisk, K. N. Clausen, and J. L. Martinez, Phys. Rev. Lett. **67**, 1791 (1991); P. Dai, H. A. Mook, and F. Dogan, *ibid.* **80**, 1738 (1998).
[28] O. Zachar, S. A. Kivelson, and V. J. Emery, Phys. Rev. B **57**, 1422 (1998).
[29] J. Zaanen, Science **286**, 251 (1999).
[30] J. M. Tranquada, J. D. Axe, N. Ichikawa, Y. Nakamura, S. Uchida, and B. Nachumi, Phys. Rev. B **54**, 7489 (1996); J. M. Tranquada, J. D. Axe, N. Ichikawa, A. R. Moodenbaugh, Y. Nakamura, and S. Uchida, Phys. Rev. Lett. **78**, 338 (1997).
[31] M. Fujita, H. Goka, K. Yamada, J. M. Tranquada, and L. P. Regnault, Phys. Rev. B **70**, 104517 (2004).
[32] S. R. White and D. J. Scalapino, Phys. Rev. Lett. **81**, 3227 (1998).
[33] G. B. Martins, R. Eder, and E. Dagotto, Phys. Rev. B **60**, R3716 (1999).
[34] The only difference between $Q^{(4)}$ and $Q^{(3)}$, is that $Q^{(4)}$ encourages horizontal stripes instead of vertical ones like $Q^{(3)}$.
[35] J. M. Tranquada, K. Nakajima, M. Braden, L. Pintschovius, and R. J. McQueeney, Phys. Rev. Lett. **88**, 075505 (2002).
[36] Since we work in finite lattices there is a discrete number of points in momentum space and additional peaks in $S(\mathbf{q})$ at val-

ues of **q** not sampled in our lattices cannot be ruled out.
[37] L. A. van Dijk, Ph.D. thesis, University of Groningen, 1998.
[38] A. Ino, C. Kim, M. Nakamura, T. Yoshida, T. Mizokawa, A. Fujimori, Z.-X. Shen, T. Kakeshita, H. Eisaki, and S. Uchida, Phys. Rev. B **65**, 094504 (2002).
[39] T. Tohyama, S. Nagai, Y. Shibata, and S. Maekawa, Phys. Rev. Lett. **82**, 4910 (1999).
[40] M. Fleck, A. I. Lichtenstein, E. Pavarini, and A. M. Oles, Phys. Rev. Lett. **84**, 4962 (2000).
[41] X. J. Zhou, P. Bogdanov, S. A. Kellar, T. Noda, H. Eisaki, S. Uchida, Z. Hussain, and Z.-X. Shen, Science **286**, 268 (1999).
[42] We have observed that the half-breathing mode induces charge inhomogeneity but not stripes.